JM PAPERS

A kind of Lagrangian chaotic property of the Arnold–Beltrami–Childress flow

Shijie Qin[1] and Shijun Liao[1,2,3],†

[1]Center of Marine Numerical Experiment, School of Naval Architecture, Ocean and Civil Engineering, Shanghai Jiao Tong University, Shanghai 200240, PR China

[2]State Key Laboratory of Ocean Engineering, Shanghai 200240, PR China

[3]School of Hydraulic Electric Engineering, Qinghai University, Xinning 810018, PR China

Three-dimensional steady-state Arnold–Beltrami–Childress (ABC) flow has a chaotic Lagrangian structure, and also satisfies the Navier–Stokes (NS) equations with an external force per unit mass. It is well known that, although trajectories of a chaotic system have sensitive dependence on initial conditions, i.e. the famous 'butterfly effect', their statistical properties are often insensitive to small disturbances. This kind of chaos (such as governed by the Lorenz equations) is called normal-chaos. However, a new concept, i.e. ultra-chaos, has been reported recently, whose statistics are unstable to tiny disturbances. Thus, ultra-chaos represents higher disorder than normal chaos. In this paper, we illustrate that ultra-chaos widely exists in Lagrangian trajectories of fluid particles in steady-state ABC flow. Moreover, solving the NS equation when $Re = 50$ with the ABC flow plus a very small disturbance as the initial condition, it is found that trajectories of nearly all fluid particles become ultra-chaotic when the transition from laminar to turbulence occurs. These numerical experiments and facts highly suggest that ultra-chaos should have a relationship with turbulence. This paper identifies differences between ultra-chaos and sensitivity of statistics to parameters. Possible relationships between ultra-chaos and the Poincaré section, ultra-chaos and ergodicity/non-ergodicity, etc., are discussed. The concept of ultra-chaos opens a new perspective of chaos, the Poincaré section, ergodicity/non-ergodicity, turbulence and their inter-relationships.

Key words: chaos

1. Introduction

The Arnold–Beltrami–Childress (ABC) flow

$$\boldsymbol{u}_{ABC}(x, y, z) = [A \sin(z) + C \cos(y)]\boldsymbol{e}_x + [B \sin(x) + A \cos(z)]\boldsymbol{e}_y$$
$$+ [C \sin(y) + B \cos(x)]\boldsymbol{e}_z \qquad (1.1)$$

† Email address for correspondence: sjliao@sjtu.edu.cn

describes a kind of stationary flow of incompressible fluid with periodic boundary conditions, where $\boldsymbol{u}_{ABC}$ is the velocity vector field, *A*, *B* and *C* are arbitrary constants, *x*, *y* and *z* are Cartesian coordinates, $\boldsymbol{e}_x$, $\boldsymbol{e}_y$ and $\boldsymbol{e}_z$ are the direction vectors of the Cartesian coordinate system, respectively. The ABC flow was first discovered by Arnold (1965) as a class of steady-state solutions of the Euler equations or the Navier–Stokes (NS) equations with external force per unit mass, and since then the Lagrangian chaotic property (Dombre *et al.* 1986; Galloway & Frisch 1986, 1987) and the so-called Beltrami property, i.e. substantial helicity $\boldsymbol{u}_{ABC} \times (\nabla \times \boldsymbol{u}_{ABC}) = 0$, of this kind of flow have aroused wide interest in nonlinear dynamics, hydrodynamics and magnetohydrodynamics.

The property of exponential deviation of a fluid particle (i.e. Lagrangian chaos) in the above-mentioned ABC flow is typical of chaotic dynamical systems (Dombre *et al.* 1986; Blazevski & Haller 2014; Didov & Uleysky 2018*a,b*) and essential for the development of turbulent flows (Dombre *et al.* 1986; Galloway & Frisch 1987; Podvigina & Pouquet 1994). This feature, in conjunction with substantial helicity, is essential for fast dynamo action (i.e. fast generation of magnetic field in conducting fluids) (Moffatt & Proctor 1985; Galloway & Frisch 1986; Finn & Ott 1988) and for the origin of magnetic field of large astrophysical objects (Childress 1970).

For a chaotic dynamical system (Li & Yorke 1975; Parker & Chua 1989; Lorenz 1993; Peter 1998; Sprott 2010; Van Gorder 2013; Lee, Borthwick & Taylor 2014; Gao *et al.* 2018), sensitivity dependence on initial conditions (SDIC) of a trajectory was first discovered by Poincaré (1890) and then rediscovered by Lorenz (1963) who proposed the popular name 'butterfly effect'. In essence, the SDIC reveals the trajectory instability of chaos. Moreover, Lorenz (1989, 2006) further discovered that the trajectories of chaotic dynamical systems have sensitive dependence not only on initial conditions (SDIC) but also on numerical algorithms (SDNA), because numerical noise, arising from truncation error and round-off error, is unavoidable for all numerical algorithms. All of these phenomena are based on the exponential increase of noise (or small disturbances), especially for the long-duration numerical simulation of a chaotic dynamical system (Ruelle & Takens 1971; Li *et al.* 2020). Naturally, the non-replicability/unreliability of chaotic trajectories has certainly led to heated debate about the credibility of numerical simulations of chaotic systems, with Teixeira, Reynolds & Judd (2007) reaching the pessimistic conclusion that 'for chaotic systems, numerical convergence cannot be guaranteed forever'.

In order to gain a reproducible/reliable numerical simulation of chaos, Liao (2009) proposed a numerical strategy, namely 'clean numerical simulation' (CNS) (Liao 2013, 2014, 2017), to greatly reduce the background numerical noise arising from truncation and round-off errors over a sufficiently long interval of time for statistical properties to be evaluated. In the frame of the CNS (Liao 2009, 2013, 2014, 2017; Liao & Wang 2014; Hu & Liao 2020; Qin & Liao 2020), spatial and temporal truncation errors are reduced to a required tiny level by means of a fine enough spatial discretization (such as the spatial Fourier expansion) and a high enough order of Taylor expansion in the temporal dimension, respectively. In particular, by using a large enough number of significant digits to represent all physical and numerical variables/parameters in multiple-precision floating-point arithmetic (Oyanarte 1990), the round-off error can be reduced to below a required tiny level. Furthermore, an additional simulation with even smaller level of background numerical noise is performed so as to determine the so-called 'critical predictable time' T_c by comparing such two simulations, so that their numerical noise (caused by truncation and round-off errors) can be negligible, i.e. several orders of magnitude smaller than the 'true' physical solution, and thus the computer-generated trajectory of chaos is reproducible/reliable within the whole spatial domain throughout the

time interval $t \in [0, T_c]$. In this way, the CNS can provide reproducible/reliable trajectories of chaotic dynamical systems in an interval of time $[0, T_c]$ that is long enough for the statistics to be evaluated properly.

The CNS provides a useful tool by which to obtain reproducible/reliable simulations of chaotic trajectory over a prescribed long time duration. To date, CNS has been successfully applied to solve many chaotic dynamical systems, such as the Lorenz equations (Liao 2009; Liao & Wang 2014), two-dimensional turbulent Rayleigh–Bénard convection (Lin, Wang & Liao 2017), chaotic motion of a disk in free fall (Xu *et al.* 2021), and certain spatiotemporal chaotic systems such as the complex Ginzburg–Landau equation (Hu & Liao 2020), the damped driven sine-Gordon equation (Qin & Liao 2020) and so on. Using CNS, more than 2000 new families of periodic orbits of Newton's (Newton 1687) three-body problem have been discovered (Li & Liao 2017; Li, Jing & Liao 2018; Li & Liao 2019), which were also reported twice in *New Scientist* (Crane 2017; Whyte 2018). It should be noted that only three families of periodic orbits of the three-body problem had been reported in the 300 years after Newton first posed the problem. Recently, comparing the CNS results (as benchmark solutions) with those given by the direct numerical simulation, Qin & Liao (2022) provided rigorous evidence that numerical noise acting as tiny artificial stochastic disturbances has both quantitative and qualitative influences on sustained turbulence. The foregoing illustrates the novelty, great potential and validity of CNS for chaotic dynamic systems.

Obviously, the numerical simulation of chaotic trajectory given by CNS can be considered as benchmark solution by which to investigate the influence of numerical noise on chaos. Using CNS, it has been found that, for certain chaotic dynamical systems, such as the Lorenz equations (Lorenz 1963), which has one positive Lyapunov exponent, and the so-called hyperchaotic Rossler system (Stankevich, Kazakov & Gonchenko 2020), which has two positive Lyapunov exponents, their statistics always remain the same under small disturbances, i.e. stable, although their trajectories are rather sensitive to small disturbances, i.e. unstable. The behaviour of such systems can be classified as normal-chaos (Liao & Qin 2022). However, the statistical properties (such as the probability density function) of some other forms of chaos are extremely sensitive to tiny noise/disturbances (Liao & Qin 2022), i.e. unstable, which is called ultra-chaos (Liao & Qin 2022; Yang, Qin & Liao 2023).

Why do we need such a new classification and such a new concept of ultra-chaos mentioned above? It is well known that numerical noise, say, truncation and round-off error, is unavoidable in numerical simulations. Thus, due to the famous butterfly effect (Lorenz 1963), numerical noise of computer-generated simulations of a chaotic system exponentially enlarges so that numerical simulations quickly become a mixture of the 'true' physical solution s and the 'false' numerical noise ε, which are mostly at the same order. Any statistics, which are calculated using such kind of mixture, are based on a hypothesis that the statistics are stable to numerical noise. In other words, the statistics based on this kind of mixture (i.e. $s + \varepsilon$) are the same as those based on the 'true' physical solution (i.e. s), say,

$$\langle s + \varepsilon \rangle = \langle s \rangle \tag{1.2}$$

must hold, where $\langle \rangle$ is a statistical operator. Here, the numerical noise ε is in fact equivalent to a kind of small disturbance. Unfortunately, there exists no theoretical proof of this hypothesis, even though it is widely utilized in many publications. Is the hypothesis (1.2) always true for all chaotic systems? The answer is unfortunately negative, according to Liao & Qin (2022), who proposed the new concept 'ultra-chaos' and classify chaos into normal-chaos and ultra-chaos, as listed in table 1 for the stability of trajectory and statistics

Type of dynamic systems	Trajectory	Statistics
Non-chaos	Stable	Stable
Normal-chaos	Unstable	Stable
Ultra-chaos	Unstable	Unstable

Table 1. Stability of trajectory and statistics of different types of dynamic systems.

of different types of dynamic systems. Such a classification of chaos is clear and easy to implement in practice. Several examples of ultra-chaos have been found in different types of chaotic systems (Liao & Qin 2022; Yang *et al.* 2023) and even in a Rayleigh–Bénard turbulent flow (Qin & Liao 2022).

In this paper, we use the unstable ABC flow (in the Lagrangian viewpoint) as an example to illustrate that ultra-chaos indeed widely exists and is in a higher disorder than a normal-chaos. Besides, we point out the essential differences between ultra-chaos and high sensitivity of statistics on certain parameters, and discuss possible relationships between ultra-chaos and ergodicity/non-ergodicity, the Poincaré section, etc. Moreover, we numerically solve the NS equation using the ABC flow plus a small disturbance as the initial condition so as to investigate the property of Lagrangian chaos of trajectories. Our results strongly suggest that turbulence should have a close relationship with ultra-chaotic trajectories, although the detailed mechanism is not yet fully understood, and thus warrants further study.

2. Ultra-chaos in the ABC flows

Let $x(t)$, $y(t)$ and $z(t)$ represent the location coordinates of a fluid particle, and $\dot{x}(t)$, $\dot{y}(t)$ and $\dot{z}(t)$ denote their temporal derivatives. Thus, in the Lagrangian sense, the motion of a fluid particle in ABC flow (1.1) is governed by

$$
\begin{cases}
\dot{x}(t) = A \sin[z(t)] + C \cos[y(t)], \\
\dot{y}(t) = B \sin[x(t)] + A \cos[z(t)], \\
\dot{z}(t) = C \sin[y(t)] + B \cos[x(t)],
\end{cases}
\tag{2.1}
$$

with the initial condition

$$
(x(0), y(0), z(0)) = \boldsymbol{r}_0,
\tag{2.2}
$$

where $\boldsymbol{r}_0$ denotes a starting point of the fluid particle. Equation (2.1) describes a typical conservative (i.e. volume-preserving) dynamical system. Without loss of generality, let us consider the case of $A = 1$ and different values of B and C. It should be emphasized here that, by means of CNS, we invariably obtain a reproducible/reliable trajectory of the chaotic motion of a fluid particle of the ABC flow over a sufficiently long interval of time. To investigate the influence of small disturbance on trajectory of the fluid particle in ABC flow (1.1) starting from $\boldsymbol{r}_0 = (x(0), y(0), z(0))$, we compare the trajectories of two close fluid particles of the ABC flow, starting from the initial positions $\boldsymbol{r}_0$ and $\boldsymbol{r}'_0 = \boldsymbol{r}_0 + (0, 0, 1) \times \delta$, respectively, where $\delta = |\boldsymbol{r}_0 - \boldsymbol{r}'_0|$ is a tiny constant. Note that $\delta = 0$ when $\boldsymbol{r}_0 = \boldsymbol{r}'_0$, corresponding to non-disturbance.

For example, without loss of generality, let us consider the motion of a fluid particle of the ABC flow (in the Lagrangian sense) starting from the point $\boldsymbol{r}_0 = (0, 0, 0)$ in the case for $A = 1$ and different values of B and C. In order to investigate its chaotic property, we compare the trajectory with that starting from a very close one $\boldsymbol{r}'_0 = \boldsymbol{r}_0 + (0, 0, 1) \times \delta$,
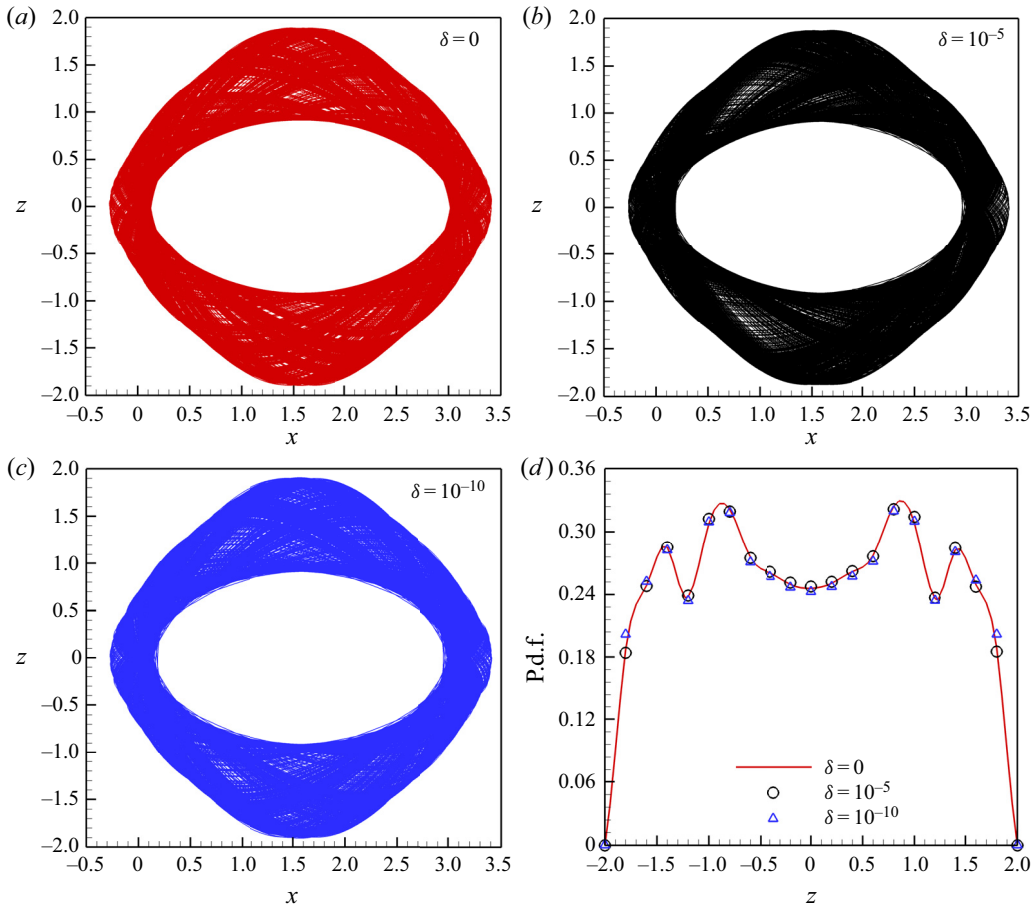
960 A15-4

Figure 1. Influence of tiny disturbances on the phase plot x–z and the probability density function (p.d.f.) of a normal-chaotic motion of a fluid particle in ABC flow. The curves are based on CNS results in $t \in [0, 10\,000]$ of a normal-chaotic fluid particle, governed by ABC flow (2.1) with (2.2) for $A = 1$, $B = 0.7$ and $C = 0.42$ (with the maximum Lyapunov exponent $\lambda_{max} = 0.01$), from the starting point $\boldsymbol{r}'_0 = (0, 0, 0) + (0, 0, 1) \times \delta$ when $\delta = 0$ (red), $\delta = 10^{-5}$ (black) and $\delta = 10^{-10}$ (blue), respectively. (*a*) Phase plot (x, z) when $\delta = 0$; (*b*) phase plot (x, z) when $\delta = 10^{-5}$; (*c*) phase plot (x, z) when $\delta = 10^{-10}$; (*d*) p.d.f.s of $z(t)$.

where we choose either $\delta = 10^{-5}$ or 10^{-10}. In each case, the chaotic simulation remains reproducible over the long interval $t \in [0, 10\,000]$ by means of a parallel algorithm of the CNS using the 200th-order Taylor expansion with the time step $\Delta t = 0.01$ and representing all data in 500-digit multiple-precision floating-point arithmetic, whose replicability/reliability is guaranteed via another CNS result with even smaller background numerical noise, given by the 205th-order Taylor expansion (with the same time step) and 520-digit multiple-precision floating-point arithmetic.

When $A = 1$, $B = 0.7$ and $C = 0.42$, a fluid particle starting from $\boldsymbol{r}_0 = (0, 0, 0)$ (corresponding to $\delta = 0$) experiences chaotic motion (with the maximum Lyapunov exponent $\lambda_{max} = 0.01$) in a restricted spatial domain, as shown in figure 1(*a*) for its phase plot (x, z) (considering the linear increase of value of y). For $\delta = 10^{-5}$ and $\delta = 10^{-10}$, although the chaotic trajectories of the two fluid particles, separately starting from the points $\boldsymbol{r}'_0$ very close to $\boldsymbol{r}_0 = (0, 0, 0)$, are rather sensitive to the starting point, their phase
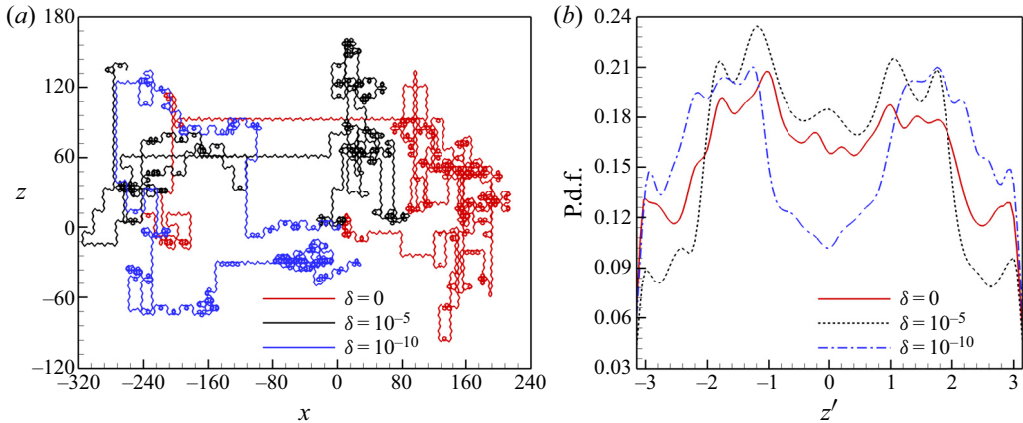
Figure 2. Influence of tiny disturbances on the phase plot x–z and the p.d.f. of an ultra-chaotic motion of a fluid particle in ABC flow. The curves are based on CNS results in $t \in [0, 10\,000]$ of an ultra-chaotic fluid particle, governed by ABC flow (2.1) with (2.2) for $A = 1.0$, $B = 0.7$ and $C = 0.43$ (with the maximum Lyapunov exponent $\lambda_{max} = 0.06$) from the starting point $r'_0 = (0, 0, 0) + (0, 0, 1) \times \delta$ when $\delta = 0$ (red), $\delta = 10^{-5}$ (black), and $\delta = 10^{-10}$ (blue), respectively. (*a*) Phase plots (x, z); (*b*) p.d.f.s of the normalized results $z'(t)$.

plots and statistical properties such as the p.d.f. are almost the same as those given by the chaotic trajectory starting from $r_0 = (0, 0, 0)$ that corresponds to $\delta = 0$, as shown in figures 1(*b*), 1(*c*) and 1(*d*), respectively. Note that here we show the p.d.f.s (as well as other statistics) only of the z-coordinate values due to the similar properties of their x-coordinate counterparts. Therefore, for $A = 1$, $B = 0.7$ and $C = 0.42$, the motion of the fluid particle starting from $r_0 = (0, 0, 0)$ is a normal-chaos, since its statistical properties such as the p.d.f. of $z(t)$ are stable, i.e. not sensitive, to a very small disturbance of the starting point.

However, for a small change in C, i.e. $\Delta C = 0.01$, such that $A = 1$, $B = 0.7$ and $C = 0.43$, the chaotic motion (with the maximum Lyapunov exponent $\lambda_{max} = 0.06$) of the fluid particle of the ABC flow starting from $r_0 = (0, 0, 0)$ becomes quite different from that for $A = 1$, $B = 0.7$ and $C = 0.42$: the fluid particle moves farther and farther away from r_0 and besides its phase plot (x, z) becomes very sensitive to the small disturbance of the starting position, as shown in figure 2(*a*). These are quite different from the results in the case of $A = 1$, $B = 0.7$ and $C = 0.42$. Since the ABC flow is periodic, we normalize the values of $z(t)$ to $[-\pi, \pi)$, i.e.

$$z'(t) = z(t) + 2\pi n_z, \tag{2.3}$$

where n_z is an integer, and $-\pi \le z' < +\pi$. Note that, as illustrated in figure 2(*b*), tiny disturbances in starting position can lead to huge deviations in the p.d.f.s of the normalized chaotic simulations $z'(t)$ in $t \in [0, 10\,000]$. In other words, for $A = 1$, $B = 0.7$ and $C = 0.43$ in the ABC flow (2.1), even statistical properties of the chaotic motion of the fluid particle starting from $r_0 = (0, 0, 0)$ are very sensitive to the initial position, and thus the corresponding motion of the particle is a kind of ultra-chaos. Obviously, this kind of ultra-chaos is at a higher level of disorder than that of the normal-chaos, as shown in figures 1 and 2. This example illustrates that ultra-chaos indeed exists in the ABC flow.

Let us further investigate some other statistics such as the variance σ^2, the kurtosis γ_2 and the ACF to demonstrate the higher disorder of the ultra-chaos than the normal-chaos mentioned above, as shown in table 2 for the normal-chaos and table 3 for the ultra-chaos. Obviously, the statistics of the normal-chaos for $C = 0.42$ (see table 2) are stable to

δ	σ^2	γ_2
0	1.2	1.8
10^{-5}	1.1	1.8
10^{-10}	1.2	1.8

Table 2. Influence of tiny disturbances (i.e. δ) on variance σ^2 and kurtosis γ_2 of the statistic results of $z(t)$ of the corresponding normal-chaotic trajectory of fluid particle in ABC flow for $A = 1$, $B = 0.7$ and $C = 0.42$. These results are obtained by solving the chaotic dynamic system (2.1) with (2.2) in $t \in [0, 10\,000]$ by means of the CNS, from the starting point $r'_0 = (0, 0, 0) + (0, 0, 1) \times \delta$ when $\delta = 0$, $\delta = 10^{-5}$ and $\delta = 10^{-10}$, respectively.

δ	σ^2	γ_2
0	2.9	1.9
10^{-5}	2.5	2.1
10^{-10}	3.4	1.6

Table 3. Influence of tiny disturbances (i.e. δ) on variance σ^2 and kurtosis γ_2 of the statistic results of $z(t)$ of the corresponding ultra-chaotic trajectory of fluid particle in ABC flow for $A = 1$, $B = 0.7$ and $C = 0.43$. These results are obtained by solving the chaotic dynamic system (2.1) with (2.2) in $t \in [0, 10\,000]$ by means of the CNS, from the starting point $r'_0 = (0, 0, 0) + (0, 0, 1) \times \delta$ when $\delta = 0$, $\delta = 10^{-5}$ and $\delta = 10^{-10}$, respectively.
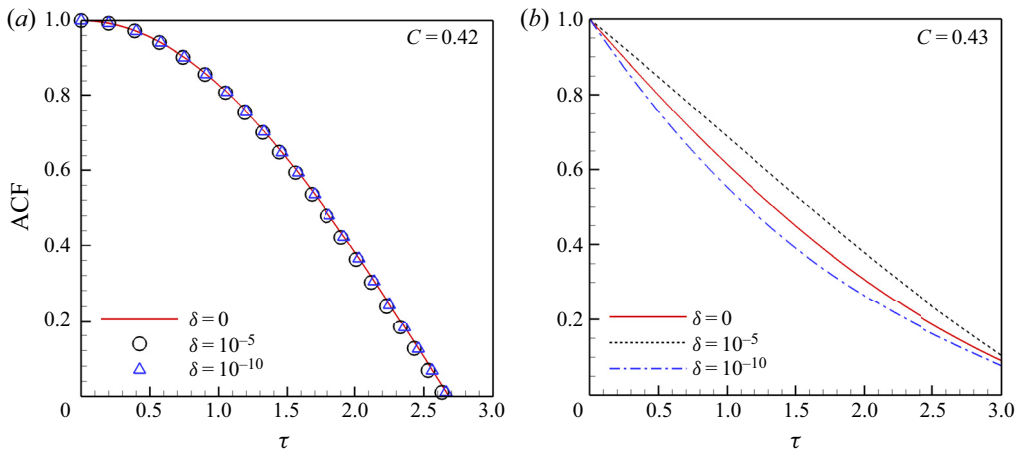

Figure 3. Influence of tiny disturbances on the autocorrelation function (ACF) of $z(t)$ of normal-chaotic or ultra-chaotic motion of a fluid particle in ABC flow. The ACFs are based on CNS results in $t \in [0, 10\,000]$ of a normal-chaotic or an ultra-chaotic fluid particle in ABC flow (2.1) with (2.2) for $A = 1$, $B = 0.7$ and either $C = 0.42$ or $C = 0.43$ from the starting point $r'_0 = (0, 0, 0) + (0, 0, 1) \times \delta$ when $\delta = 0$ (red), $\delta = 10^{-5}$ (black) and $\delta = 10^{-10}$ (blue), respectively. (*a*) Variation in ACF with τ of normal-chaotic particle when $C = 0.42$, and (*b*) variation in ACF with τ of ultra-chaotic particle when $C = 0.43$, where τ denotes the lag.

small disturbances. Conversely, the statistics of ultra-chaos for $C = 0.43$ (see table 3) are sensitive to tiny disturbances and thus unstable. In addition, the ACF of the ultra-chaos is also sensitive to small disturbances, compared with that of the normal-chaos, as shown in figure 3.
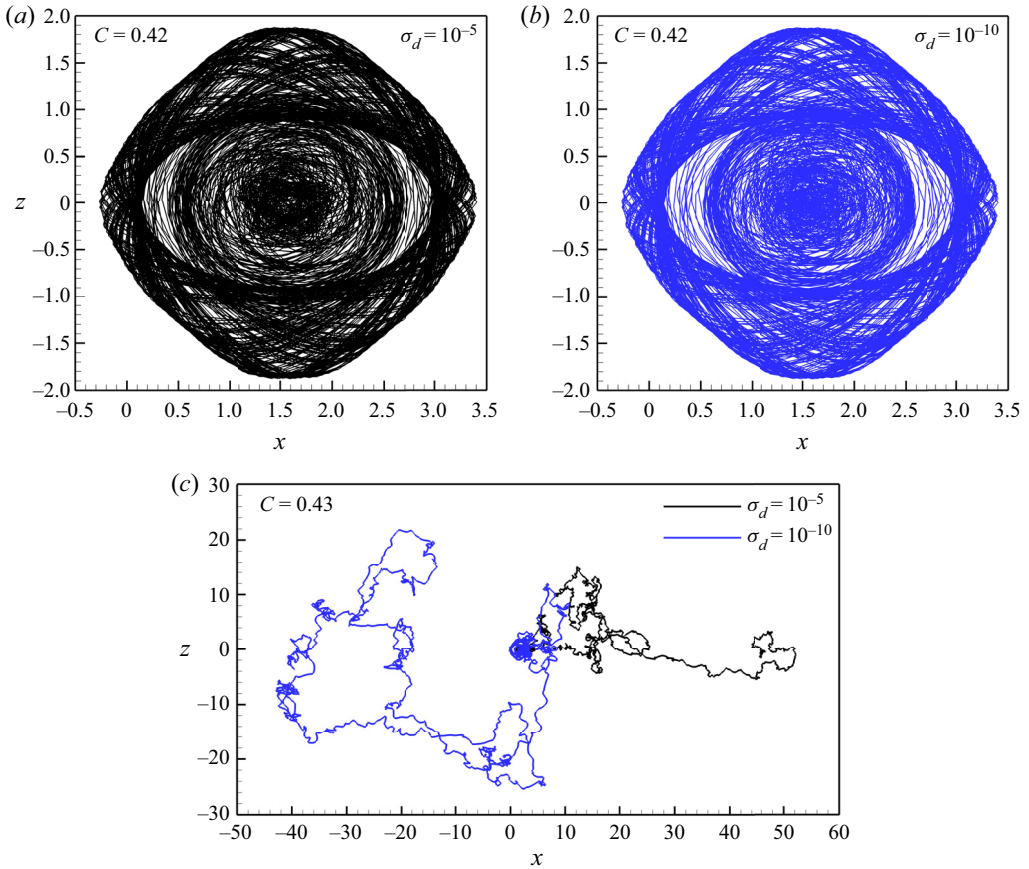
Figure 4. Influence of tiny disturbances on the x–z phase plot of ensemble-averaged trajectory of a normal-chaotic ($C = 0.42$) or an ultra-chaotic ($C = 0.43$) fluid particle in ABC flow (2.1) for $A = 1$ and $B = 0.7$. They are based on CNS results in $t \in [0, 10\,000]$ from the starting point $r_0 = (0, 0, 0) + (0, 0, 1) \times \delta_i$, $1 \le i \le 1000$, with $\sigma_d = \sqrt{\langle \delta_i^2 \rangle} = 10^{-5}$ (black) and $\sigma_d = 10^{-10}$ (blue), respectively. (*a*) The x–z phase-plot of the normal-chaotic fluid particle when $C = 0.42$ with $\sigma_d = 10^{-5}$; (*b*) the x–z phase-plot of the normal-chaotic fluid particle with $\sigma_d = 10^{-10}$; (*c*) the x–z phase-plot of the ultra-chaotic fluid particle when $C = 0.43$ with either $\sigma_d = 10^{-5}$ or 10^{-10}.

   Furthermore, let us consider the ensemble average of chaotic trajectories of a fluid particle starting from the point $r'_0 = r_0 + (0, 0, 1) \times \delta_i$ with 1000 different tiny disturbances δ_i ($i = 1, 2, 3, \ldots, 1000$), which are given by the Gaussian random number generator with a standard deviation $\sigma_d = \sqrt{\langle \delta_i^2 \rangle}$ and a zero mean, i.e. $\mu_d = \langle \delta_i \rangle = 0$, where $\langle \rangle$ denotes the average operator. For $A = 1$, $B = 0.7$ and $C = 0.42$ and $r_0 = (0, 0, 0)$, corresponding to the normal-chaotic motions of a fluid particle, the ensemble averages of the phase plots x–z, which are given, respectively, either by $\sigma_d = 10^{-5}$ or $\sigma_d = 10^{-10}$, are almost the same, as shown in figures 4(*a*) and 4(*b*). On the contrary, for $A = 1$, $B = 0.7$ and $C = 0.43$, the ensemble averages of the phase plots x–z (of the ultra-chaotic motions of a fluid particle), which are given by either $\sigma_d = 10^{-5}$ or $\sigma_d = 10^{-10}$, are totally different, as shown in figure 4(*c*). Furthermore, the p.d.f. of the ensemble-averaged trajectory of the ultra-chaotic fluid particle starting from r'_0 is also very sensitive to the standard deviation σ_d of the starting position, which is completely different from that given by the
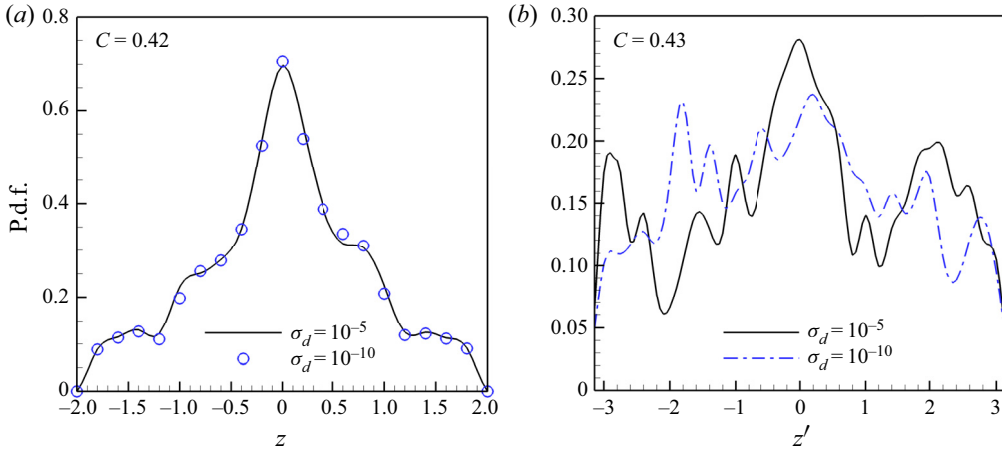
960 A15-8

Figure 5. Influence of tiny disturbances on the p.d.f. of ensemble-averaged trajectory of a normal-chaotic ($C = 0.42$) or an ultra-chaotic ($C = 0.43$) fluid particle in ABC flow (2.1) with (2.2) for $A = 1$ and $B = 0.7$. The p.d.f.s of the ensemble-averaged trajectories are based on the CNS results in $t \in [0, 10\,000]$ from the starting point $\boldsymbol{r}_0 = (0, 0, 0) + (0, 0, 1) \times \delta_i$, $1 \le i \le 1000$, with $\sigma_d = \sqrt{\langle \delta_i^2 \rangle} = 10^{-5}$ (black) and $\sigma_d = 10^{-10}$ (blue), respectively. (*a*) The p.d.f.s of $z(t)$ of the normal-chaotic fluid particle when $C = 0.42$; (*b*) the p.d.f.s of the normalized results $z'(t)$ of the ultra-chaotic fluid particle when $C = 0.43$.

normal-chaotic fluid particle, as illustrated in figure 5. These results indicate that, unlike a normal-chaos, even ensemble-averaged quantities and their corresponding p.d.f.s for an ultra-chaos in ABC flow are unstable, i.e. rather sensitive to tiny disturbances. Indeed, the ultra-chaotic motion is at a higher level of disorder than that of a normal-chaos in ABC flow.

It should be emphasized that the main characteristic of ultra-chaos is that some statistics such as p.d.f. are extremely sensitive to tiny disturbances (Liao & Qin 2022). Thus, in this paper we analyse the influence of tiny disturbances in starting position on the chaotic motions of fluid particles in ABC flow. According to the results mentioned above, other statistical properties (such as variance, kurtosis, ACF, ensemble-averaged trajectory and ensemble-averaged trajectory's p.d.f.) of ultra-chaos in the ABC flow are also very sensitive to tiny disturbances in the starting position. On the contrary, these statistics, given by CNS results of a normal-chaotic fluid particle in the ABC flow, are not sensitive to tiny disturbances. This indicates that the statistics of a normal-chaos are stable.

For $A = 1$ and varying the values of B and C, we find that non-chaos, normal-chaos and ultra-chaos all exist in the fluid particle trajectory starting from $\boldsymbol{r}_0 = (0, 0, 0)$, as shown in figure 6. For a non-chaotic motion, the fluid particle trajectory is stable to tiny disturbances in the starting position. For a normal-chaotic motion, although the trajectory is rather sensitive to tiny disturbances in the starting position, i.e. unstable, the phase plot and the statistical properties are stable to the tiny disturbances. However, for an ultra-chaotic motion, even the statistical properties are unstable, say, sensitive to tiny disturbances in the starting position. As we can see in figure 6, for $A = 1$ and $B = 0.7$, a small change between $C = 0.42$ and $C = 0.43$ triggers the transition from normal-chaotic motion to ultra-chaotic motion, which is the reason why we present the cases in figures 1 and 2. Note that for the normal-chaotic motion, the fluid particle starting from $\boldsymbol{r}_0 = (0, 0, 0)$ always moves in a restricted spatial domain (such that its position is in a restricted domain of the phase plot x–z as shown in figure 1). However, for an ultra-chaotic motion, the fluid
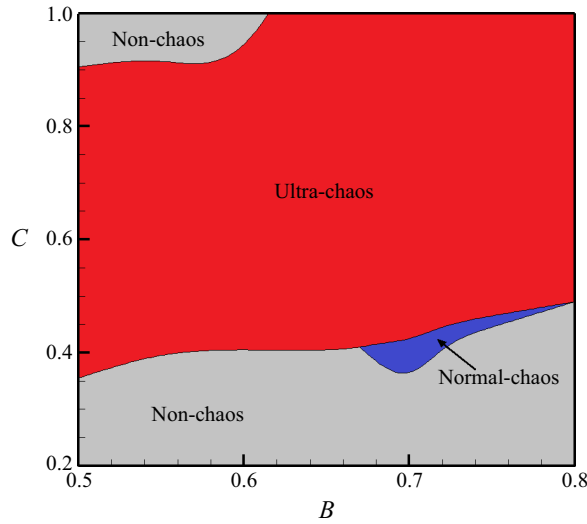
Figure 6. Classification of trajectories of fluid particles in ABC flow (2.1) starting from $r_0 = (0, 0, 0)$ for different values of B and C when $A = 1$: grey domain, non-chaos; blue domain, normal-chaos; red domain, ultra-chaos.

particle starting from $r_0 = (0, 0, 0)$ progressively departs from its starting point, further illustrating that ultra-chaotic motion in ABC flow has higher disorder than normal-chaotic motion, although the velocity field of the ABC flow as a whole is inherently periodic and steady-state.

On the other hand, keeping $A = 1$, $B = 0.7$ and $C = 0.43$ and using various positions of the starting point $r_0 = (x(0), y(0), z(0))$ in ABC flow, where $-\pi \leq x(0), y(0), z(0) \leq +\pi$, it is found in a similar way that both normal-chaos and ultra-chaos (for the motions of fluid particles starting from different r_0) widely exist, and these two states of chaos coexist simultaneously in the ABC flow, as shown in figure 7. The statistical values of their maximum Lyapunov exponents λ_{max} are given in table 4. Statistically speaking, the maximum Lyapunov exponents λ_{max} of the ultra-chaotic motions of fluid particles in ABC flow are approximately two orders of magnitude larger than those of the normal-chaos.

Note that, when $z(0)$ of the starting point $r_0 = (x(0), y(0), z(0))$ increases from 0 to $\pi/2$, there exists a kind of structure constituted by the starting positions $(x(0), y(0))$ of fluid particles with normal-chaotic motion (corresponding to blue points) and ultra-chaotic motion (red points), which undergoes continuous deformation, as shown in figure 7. Although normal-chaotic motion is qualitatively different from ultra-chaotic motion so that it is not difficult for us to obtain the general structure in figure 7, we still require a criterion by which to quantitatively determine the boundary of the structure. Let $f(z')$ denote the p.d.f. of a normalized result $z' \in [-\pi, +\pi)$ given by a chaotic motion of fluid particle, and $f^*(z')$ the p.d.f. of another one with a tiny disturbance to the starting position. A criterion based on the following relative error:

$$\frac{\int_{-\pi}^{+\pi} |f(z') - f^*(z')| \, dz'}{\int_{-\pi}^{+\pi} f(z') \, dz'} = \int_{-\pi}^{+\pi} |f(z') - f^*(z')| \, dz' \leq \gamma \quad (2.4)$$
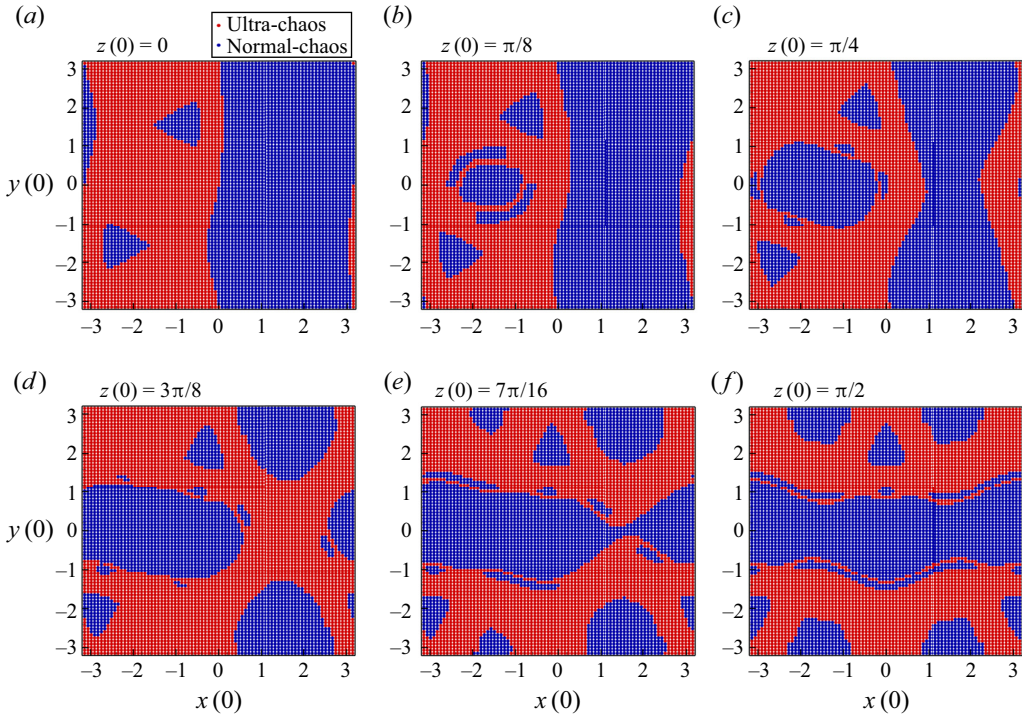
960 A15-10

Figure 7. Chaotic states of trajectories of the fluid particles starting from different points $r_0 = (x(0), y(0), z(0))$ in ABC flow (2.1) for $A = 1$, $B = 0.7$ and $C = 0.43$. Here (*a*) $z(0) = 0$; (*b*) $z(0) = \pi/8$; (*c*) $z(0) = \pi/4$; (*d*) $z(0) = 3\pi/8$; (*e*) $z(0) = 7\pi/16$; (*f*) $z(0) = \pi/2$. Blue points, normal-chaos; red points, ultra-chaos.

	Normal-chaos	Ultra-chaos
Maximum value of λ_{max}	1.3×10^{-2}	8.7×10^{-2}
Minimum value of λ_{max}	8.5×10^{-5}	4.3×10^{-2}
Mean of λ_{max}	9.7×10^{-4}	6.9×10^{-2}
Standard deviation of λ_{max}	7.5×10^{-4}	1.0×10^{-2}

Table 4. Statistical values of maximum Lyapunov exponents λ_{max} of the normal-chaotic and ultra-chaotic trajectories of fluid particles in the ABC flow, gained by solving the chaotic dynamic system ABC flow (2.1) in $t \in [0, 10\,000]$ for $A = 1$, $B = 0.7$ and $C = 0.43$ by means of CNS, using various starting points $r_0 = (x(0), y(0), z(0))$ of the fluid particles, where $-\pi \leq x(0), y(0), z(0) \leq +\pi$.

is usually adopted to determine the boundary between normal-chaos and ultra-chaos, as shown in figure 7. According to our experience, $\gamma = 5\%$ is often suitable to distinguish between a normal-chaotic motion and an ultra-chaotic motion. Figure 7 illustrates that the normal-chaotic and ultra-chaotic states coexist at the same time, which is reasonable in a volume-preserving ABC flow that has different types of chaotic trajectories for the motions of fluid particles (Dombre *et al.* 1986), which will be discussed later in detail.

Let $\alpha(x(0), y(0), z(0)) = 0$ or 1 denote either a normal-chaotic motion or an ultra-chaotic motion of a fluid particle starting from $r_0 = (x(0), y(0), z(0))$, respectively.

Then, according to our computations, for $-\pi \leq x(0) \leq +\pi$, there exist the symmetries

$$\alpha(x(0), y(0), z(0)) = \alpha(-x(0), y(0), \pi - z(0)), \tag{2.5}$$

where $y(0) \in [-\pi, +\pi]$, $z(0) \in [\pi/2, \pi]$;

$$\alpha(x(0), y(0), z(0)) = \alpha(x(0), \pi - y(0), -z(0)), \tag{2.6}$$

where $y(0) \in [0, \pi]$, $z(0) \in [-\pi, 0]$; and

$$\alpha(x(0), y(0), z(0)) = \alpha(x(0), -\pi - y(0), -z(0)), \tag{2.7}$$

where $y(0) \in [-\pi, 0]$, $z(0) \in [-\pi, 0]$, respectively.

Considering the fact that the normal-chaotic and ultra-chaotic states coexist simultaneously as shown in figure 7, without loss of generality, we choose two starting points $r_{0,n} = (0, -0.1, 0)$ and $r_{0,u} = (-0.1, 0.1, 0)$ of fluid particles in ABC flow to illustrate a normal-chaotic motion (left) and an ultra-chaotic motion (right) via a movie (see the supplementary movie available at https://doi.org/10.1017/jfm.2023.190) in the case of $A = 1$, $B = 0.7$, $C = 0.43$ within $t \in [0, 5000]$. As shown in the left part of the movie (corresponding to a normal-chaos), the fluid particle starting from $r_{0,n}$ always moves in a restricted spatial domain and the corresponding trajectory resembles weak chaos. On the contrary, the fluid particle starting from $r_{0,u}$ departs the starting point far away and even its position normalized by periodic condition appears to be in disorder, as shown in the right part of the movie (corresponding to ultra-chaos). All of these clearly illustrate that an ultra-chaotic motion in the ABC flow is completely different from a normal-chaotic motion: an ultra-chaos has indeed a much higher disorder than a normal-chaos.

Let β denote the ratio of the number of the starting fluid particles with ultra-chaotic motion to the total number of particles in $-\pi \leq x, y, z \leq +\pi$. In theory

$$\beta = \frac{1}{(2\pi)^3} \int_{-\pi}^{+\pi} \int_{-\pi}^{+\pi} \int_{-\pi}^{+\pi} \alpha(x, y, z) \, dx \, dy \, dz, \tag{2.8}$$

with either $\alpha = 0$ for a normal-chaos or $\alpha = 1$ for an ultra-chaos, respectively. In practice, we use the Monte-Carlo method to estimate the ratio

$$\beta \approx \frac{N_{ultra}}{N_{all}}, \tag{2.9}$$

where N_{all} denotes the total number of the randomly selected starting fluid particles

$$r_0 \in \Omega = \{(x, y, z) : -\pi \leq x, y, z \leq +\pi\} \tag{2.10}$$

and N_{ultra} is the number of starting fluid particles with ultra-chaotic motion. Obviously, the larger N_{all}, the more accurate the result of β given by the Monte-Carlo method. For $A = 1$, $B = 0.7$, $0 \leq C \leq 0.43$ and $N_{all} = 8000$, it is found that the ratio β is dependent upon the value of C, as shown in table 5. Notably, when $C \leq 0.1$, it is found that there exists a power-law relationship between β and C, say,

$$\beta \approx C^{0.4}, \tag{2.11}$$

as illustrated in figure 8. Thus, when the parameter C decreases, the value of N_{ultra}, i.e. the number of the starting fluid particles with ultra-chaotic motion, decreases until $N_{ultra} = 0$ when $C = 0$. This is reasonable since the ABC flow for $C = 0$ is stable and thus chaotic motion of fluid particles does not exist at all in $C = 0$.

960 A15-12

C	N_{ultra}/N_{all}
0.43	49 %
0.2	47 %
0.1	43 %
0.01	20 %
0.001	6 %
0.0001	2 %
0	0 %

Table 5. Values of the parameter C versus N_{ultra}/N_{all}, where N_{ultra} denotes the number of starting points corresponding to an ultra-chaotic trajectory of fluid particle in the ABC flow and N_{all} denotes the total number of equidistant starting points. The results are obtained by solving the chaotic dynamical system (2.1) in $t \in [0, 10\,000]$ for $A = 1.0$, $B = 0.7$ and $0 \le C \le 0.43$ by means of CNS, using various starting points $\boldsymbol{r}_0 = (x(0), y(0), z(0))$ of the fluid particles, where $-\pi \le x(0), y(0), z(0) \le +\pi$.
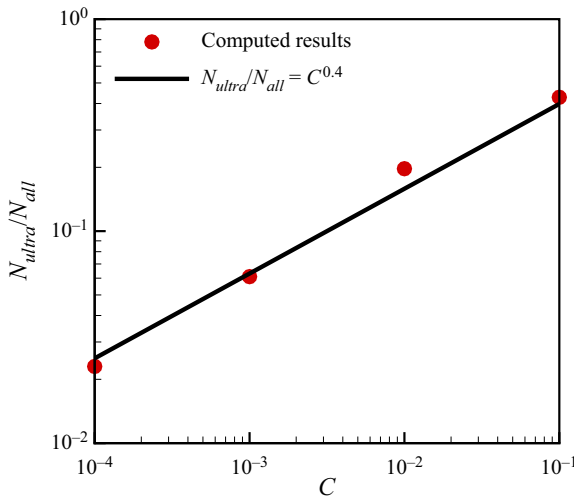

Figure 8. The ratio of the number of the starting fluid particles with ultra-chaotic motion to the total number of particles versus the value of C of ABC flow for $A = 1$, $B = 0.7$ and $C \le 0.1$.

2.1. *Difference between ultra-chaos and sensitivity of statistics to parameters*

It is well known that a chaotic trajectory is unstable, i.e. sensitive to small disturbances. For normal-chaos, a trajectory is unstable but its statistics are stable to small disturbances. However, for ultra-chaos, even its statistics are unstable, i.e. sensitive to very small disturbances. The stability of different types of dynamic system is listed in table 1. Obviously, as illustrated by many examples (Liao & Qin 2022; Yang *et al.* 2023), ultra-chaos involves higher disorder than normal-chaos.

It should be emphasized that, unlike sensitivity to parameters, the concept of ultra-chaos focuses on the stability of statistics of a dynamic system, while all physical parameters are fixed, to small disturbances that can be very tiny. Certain dynamic systems exhibit high sensitivity in statistics to physical parameters (Broer, Simó & Vitolo 2002; Ashwin *et al.* 2012; Lucarini & Bódai 2019; Śliwiak, Chandramoorthy & Wang 2021), which, however, is essentially different from ultra-chaos, i.e. instability of statistics to small disturbances. For example, Broer *et al.* (2002) investigated bifurcations and strange attractors in the

Lorenz-84 climate model with seasonal forcing,

$$\dot{x} = -ax - y^2 - z^2 + aF\left(1 + \epsilon \cos \omega t\right), \tag{2.12}$$

$$\dot{y} = -y + xy - bxz + G\left(1 + \epsilon \cos \omega t\right), \tag{2.13}$$

$$\dot{z} = -z + bxy + xz, \tag{2.14}$$

where $\omega = 2\pi/T$ and a, b, T, F, G, ϵ are physical parameters. Without loss of generality, Broer *et al.* (2002) considered the cases of $a = 1/4, b = 4, T = 73$ with varying $F \in [0, 12], G \in [0, 9]$ and $\epsilon \in [0, 0.5]$, and found that there exist Hopf bifurcations and some high sensitivity of statistics to parameters F, G and ϵ. However, we found that all statistic results given by the above-mentioned Lorenz-84 climate model with seasonal forcing are stable to small disturbances, in that they are either non-chaotic or normal-chaotic. In other words, even when high sensitivity of statistics to physical parameters exists, the corresponding dynamic system is stable and thus is not an ultra-chaos! In fact, like the famous three-dimensional Lorenz equation (with one positive Lyaponov exponent) and the four-dimensional Rössler system (with two positive Lyaponov exponents) (Liao & Qin 2022), the above-mentioned Lorenz-84 climate model has normal-chaotic trajectories at most. This is a good example to illustrate the essential difference between ultra-chaos and high sensitivity of statistics to physical parameters: they are quite different things!

For an ultra-chaotic system, its statistics are unstable to any types of disturbances. For example, in the case of $A = 1$, $B = 0.7$ and $C = 0.43$, the trajectory starting from $(0, 0, 0)$ is still ultra-chaotic even if there is no disturbance to the starting point but a small environmental disturbance, governed by

$$\begin{cases} \dot{x}(t) = A \sin[z(t)] + C \cos[y(t)], \\ \dot{y}(t) = B \sin[x(t)] + A \cos[z(t)], \\ \dot{z}(t) = C \sin[y(t)] + B \cos[x(t)] + \varepsilon(t), \end{cases} \tag{2.15}$$

with the initial condition

$$(x(0), y(0), z(0)) = \boldsymbol{r}_0, \tag{2.16}$$

where $\varepsilon(t)$ is a normally random noise with a small standard deviation (at the order of magnitude 10^{-10}), and $\boldsymbol{r}_0$ is the starting point, respectively. We found that, even for the fixed values of $A = 1, B = 0.7, C = 0.43$ and the exact starting position $\boldsymbol{r}_0 = (0, 0, 0)$, the statistics of the corresponding trajectory are unstable, i.e. rather sensitive to the normally random noise $\varepsilon(t)$. In this case, the trajectory is ultra-chaotic, but there exists no sensitivity of statistics to parameters, because the starting position and all physical parameters have exactly the same values. This further indicates the essential differences between ultra-chaos and sensitivity of statistics to parameters.

2.2. *Possible relationship between ultra-chaos and Poincaré section*

Following Dombre *et al.* (1986), we obtain the Poincaré section of the ABC flow (2.1) for $A = 1, B = 0.7$ and $C = 0.43$, as shown in figure 9. Here, we applied CNS to obtain the trajectories $(x(t), y(t), z(t))$ of fluid particles in $t \in [0, 10\,000]$, starting from several selected points (listed in table 6). For each trajectory, we have a point (x', y') when $z'(t) = 2n\pi$ for an arbitrary integer n, corresponding to a point (x^*, y^*) in the square domain

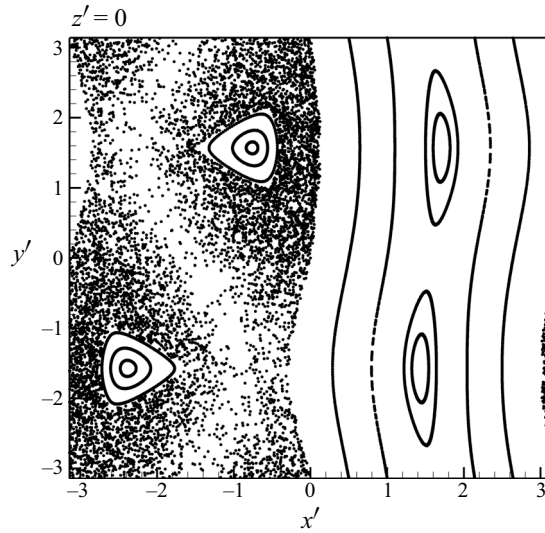$$x^* \in [-\pi, +\pi), \quad y^* \in [-\pi, +\pi), \tag{2.17a,b}$$

Figure 9. Poincaré section at $z' = 0$ for several normalized trajectories $(x'(t), y'(t), z'(t))$ in $t \in [0, 10\,000]$ of fluid particles starting from different points $\boldsymbol{r}_0 = (x(0), y(0), z(0))$ (as listed in table 6) obtained by means of CNS for ABC flow (2.1) in the case of $A = 1$, $B = 0.7$ and $C = 0.43$.

Starting point	x(0)	y(0)
No. 1	0	0
No. 2	−0.1	0
No. 3	−0.2	0
No. 4	−0.3	0
No. 5	−0.4	0
No. 6	−0.5	0
No. 7	−0.6	0
No. 8	−0.7	0
No. 9	−0.8	0
No. 10	−0.9	0
No. 11	−1.0	0
No. 12	−1.5	0
No. 13	0.5	0
No. 14	1.0	0
No. 15	1.5	1.5
No. 16	1.6	1.6
No. 17	−1.8	−1.5
No. 18	−2.1	−1.5
No. 19	−2.3	−1.5
No. 20	−0.8	1.5
No. 21	−1	1.5
No. 22	−1.3	1.5

Table 6. Positions $\boldsymbol{r}_0 = (x(0), y(0), 0)$ of the starting particles, chosen for the Poincaré section shown in figure 9.

by means of the periodic condition in x' and y' directions, say,

$$x' = x^* + 2m\pi, \quad y' = y^* + 2k\pi, \qquad (2.18a,b)$$

where *m* and *k* are integers. The set of all these points (x^*, y^*) gives the Poincaré section of the ABC flow (2.1), as shown in figure 9. For details, please refer to Dombre *et al.* (1986).

As shown in figure 9, there exist elliptic islands (or Kolmogorov–Arnold–Moser (KAM) tori) and a chaotic sea in the Poincaré section. By convention, it is widely believed that points in an elliptic island correspond to quasiperiodic orbits or weakly chaotic orbits, but points in a chaotic sea correspond to strongly chaotic orbits, respectively (Kuznetsov & Zaslavsky 2000; Skokos 2001; Lukes-Gerakopoulos, Voglis & Efthymiopoulos 2008). Interestingly, the Poincaré section (as shown in figure 9) is rather similar to figure 7(*a*). So, it is reasonable for particles starting from the elliptic islands (or KAM tori) to represent a kind of normal-chaotic property, because their maximum Lyapunov exponents $8.5 \times 10^{-5} \leq \lambda_{max} \leq 1.3 \times 10^{-2}$ (listed in table 4) indeed correspond to a weak chaos. This numerical fact reveals the following relationship: the normal-chaotic (starting) points (at $z = 0$) of the ABC flow correspond to the elliptic islands (or KAM tori) in the Poincaré section, but the ultra-chaotic ones invariably correspond to the chaotic sea. According to our computations, this kind of relationship is true for almost all fluid particles in the ABC flow. Besides, this numerical experiment also supports our conclusion that an ultra-chaos is a higher disorder than a normal-chaos. Thus, the classification of chaos into normal-chaos and ultra-chaos provides a new explanation of elliptic islands (or KAM tori) and chaotic sea in Poincaré section of a dynamic system.

Note that Poincaré section has a close relationship with KAM theory that is valid for an integrable Hamiltonian system only. However, the classification of chaos into ultra-chaos and normal-chaos is generally valid for all dynamic systems, even if they are not Hamiltonian, or not integrable. Therefore, this classification has a more general meaning, given that ultra-chaos reveals higher disorder than normal-chaos. An example of such higher disorder related to statistical sensitivity to small disturbances has been recently reported: small disturbances can lead to large-scale deviations of simulations of a turbulent flow not only in spatiotemporal trajectories but also in statistics, even leading to different types of flow (Qin & Liao 2022).

2.3. *Possible relationship between ultra-chaos and ergodicity/non-ergodicity*

According to our numerical experiments mentioned above, statistics are stable for a normal-chaotic motion of fluid particles in the ABC flow, but unstable for an ultra-chaotic motion of fluid particles in the same ABC flow. However, it is an open question whether or not a normal-chaos should correspond to ergodicity and an ultra-chaos to non-ergodicity, because it is rather difficult in practice to prove ergodicity or non-ergodicity of a dynamic system.

According to Birkhoff (1931) and von Neumann (1932), time averages can be set equal to phase averages, provided the system is ergodic, i.e. metrically transitive (Moore 2015). However, it is difficult to prove conclusively that a system is metrically transitive. In fact, Birkhoff (1931) and von Neumann (1932) did not actually solve the problem of equating time averages and phase averages but instead reduced it to an equally difficult problem of proving metric transitivity, as pointed out by Moore (2015). For example, in the case of $A = 1$, $B = 0.7$ and $C = 0.43$, our computations clearly indicate that a fluid particle starting from $r_{0,n} = (0, -0.1, 0)$ has a normal-chaotic trajectory, but another fluid particle starting from $r_{0,u} = (-0.1, 0.1, 0)$ has an ultra-chaotic trajectory, as shown in the movie. How can we prove that, under the same velocity field u_{ABC} of the ABC flow, the trajectory of the former particle is metrically transitive (i.e. ergodic) but the latter is not (i.e. non-ergodic)? From a practical viewpoint, it is much easier for us to conclude

that the former trajectory is normal-chaotic whereas the latter trajectory is ultra-chaotic by investigating the stability of its statistical properties via time average (or ensemble average) than to prove (or disprove) its metric transitivity for ergodicity, since either time or ensemble averaging is quite easy. Therefore, from a practical point of view, ultra-chaos is a more useful concept than non-ergodicity!

It would be very convenient if one could theoretically prove (or disprove) that every ergodic system corresponds to a normal-chaos and every non-ergodic system to an ultra-chaos, respectively. If so, the classification of normal-chaos and ultra-chaos might provide us with a simple and practical way to reveal ergodic properties of various types of dynamic systems, given that it is much easier to check stability of statistics through spatio-temporal average (or ensemble average) than to prove (or disprove) metric transitivity.

3. Possible relationship between ultra-chaos and turbulence

The velocity $\boldsymbol{u}_{ABC}$ of the ABC flow (1.1) was first discovered by Arnold (1965) as a class of steady-state solutions of the Euler equations, and, moreover, with external force per unit mass, it also satisfies the NS momentum and continuity equations

$$\frac{\partial \boldsymbol{u}}{\partial t} + (\boldsymbol{u} \cdot \nabla)\boldsymbol{u} = -\nabla p + \frac{1}{Re}\Delta \boldsymbol{u} + \boldsymbol{f}, \tag{3.1}$$

$$\nabla \cdot \boldsymbol{u} = 0, \tag{3.2}$$

where $t \geq 0$ denotes the time, ∇ is the Hamilton operator, Δ is the Laplace operator, Re is the Reynolds number, p denotes the pressure and

$$\boldsymbol{f} = \frac{\boldsymbol{u}_{ABC}}{Re} \tag{3.3}$$

is the given external force per unit mass, with the periodic boundary conditions at $x = \pm\pi$, $y = \pm\pi$, and $z = \pm\pi$.

Many papers (Dombre *et al.* 1986; Mezić 2002; Podvigina, Ashwin & Hawker 2006) have been published in this field. For example, Podvigina *et al.* (2006) analysed the bifurcation of the ABC flow and reported the supercritical Hopf bifurcation and route to chaos through tori doubling. Without loss of generality, let us consider here the ABC flow in the case of $A = 1$, $B = 0.7$ and $0 \leq C \leq 0.43$. Unlike other researchers (Dombre *et al.* 1986; Mezić 2002; Podvigina *et al.* 2006), here we mainly focus on the ultra-chaotic motion of fluid particles. As reported by Podvigina & Pouquet (1994), the Reynolds number $Re = 50$ corresponds to a turbulent flow if the initial velocity field $\boldsymbol{u}_{ABC}$ experiences small disturbances of the order of magnitude 10^{-3}. This kind of turbulent flow is solved numerically in $t \in [0, 500]$: the spatial domain $[-\pi, +\pi)^3$ is discretized by a uniform mesh with 128^3 points for the spatial Fourier expansion, where the maximum grid spacing is less than the minimum Kolmogorov scale (Pope 2001), and the 3/2 rule for dealiasing (Pope 2001) is used, with the time step $\Delta t = 10^{-3}$.

First, let us use the unstable ABC flow for $A = 1.0$, $B = 0.7$ and $C = 0.43$ as the initial condition of the NS equations (3.1) and (3.2) (with the external force per unit mass $\boldsymbol{f} = \boldsymbol{u}_{ABC}/Re$ as mentioned above), under small disturbances of initial velocity at the order of magnitude 10^{-3}. It is found that, the flow is initially rather similar to the ABC flow at times that are too short for the tiny velocity disturbances to transfer to the macrolevel; in this situation, approximately 49 % starting fluid particles are ultra-chaotic, according to table 5. The transition from laminar flow to turbulence occurs approximately at $t \approx 50.0 = T_{tran}$,
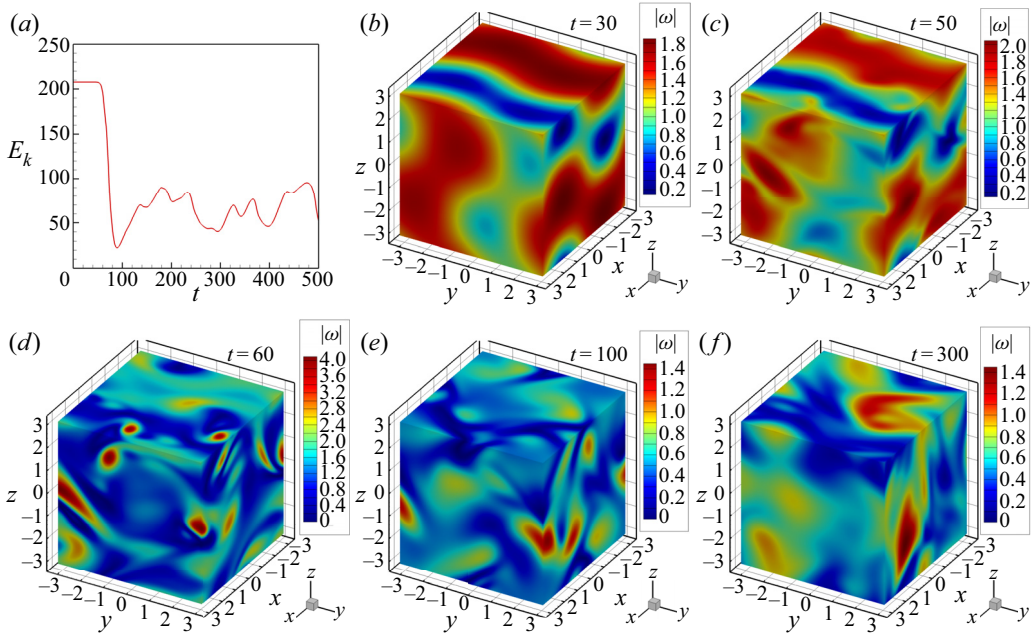
Figure 10. (*a*) Total kinetic energy; (*b*–*f*) modulus $|\boldsymbol{\omega}|$ of instantaneous vorticity field at $t = 30$, $t = 50$, $t = 60$, $t = 100$, or $t = 300$, respectively, governed by the NS equations (3.1) and (3.2) with $R_e = 50$ using the ABC flow (1.1) (for $A = 1$, $B = 0.7$ and $C = 0.43$) under a small disturbance at the order of magnitude 10^{-3} as the initial solution.

as shown in figure 10, where T_{tran} denotes the time of the transition occurrence. Given the velocity field $\boldsymbol{u}$ of (3.1) and (3.2), we can investigate the chaotic property of trajectory (i.e. whether it is ultra-chaotic or normal-chaotic) of a fluid particle starting from $\boldsymbol{r}_0$ in a similar way as mentioned in § 2. When $t = 50$, we randomly choose 10 000 starting fluid particles in $-\pi \leq x, y, z < +\pi$ and find that all trajectories of the fluid particles starting from them are ultra-chaotic. This numerical experiment strongly suggests that a necessary condition of turbulence is that almost all fluid particles should move along ultra-chaotic trajectories.

Similarly, let us consider the stable ABC flow in the case of $A = 1$, $B = 0.7$ and $C = 0$. Using the ABC flow $\boldsymbol{u}_{ABC}$ subject to small disturbances at the order of magnitude 10^{-3} as the initial condition, we numerically solve the NS and continuity equations (3.1) and (3.2) in the time interval $t \in [0, 2000]$ and investigate the chaotic property of trajectories of the 10 000 randomly chosen fluid particles. It is found that, when $C = 0$, transition from the laminar flow to turbulence never occurs, and, moreover, there exists no ultra-chaotic motion for all of these fluid particles throughout $t \in [0, 2000]$. This further confirms our suggestions that ultra-chaotic trajectories of fluid particles should have some relationships with turbulence.

In addition, let us further consider the ABC flows for $A = 1$, $B = 0.7$ and different values of C, and for each case we use the Monte-Carlo method to randomly choose 10 000 starting points in $-\pi \leq x, y, z < +\pi$. It is found that the transition time T_{tran} when the flow alters from laminar flow to turbulence increases as C decreases from 0.1 to 0.0001, as shown in table 7. We found that, when $0 < C \leq 0.1$, there exists a linear relationship

$$T_{tran} \approx -10 \log_{10}(C) + 40, \qquad (3.4)$$

C	T_{tran}
0.1	50.5
0.01	59.5
0.001	70.0
0.0001	80.0
0.0	—

Table 7. Transition occurrence time T_{tran} for different values of C, gained by numerically solving the NS equations (3.1) and (3.2) using the ABC flow (1.1) (for $A = 1$, $B = 0.7$ and $0 \leq C \leq 0.1$) as the initial condition plus a small disturbance of velocity field at the order of magnitude 10^{-3}.
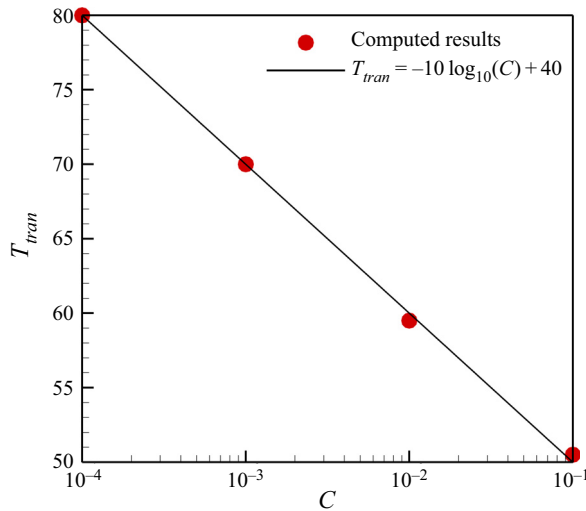

Figure 11. Relationship between C and T_{tran} obtained for ABC flow with $A = 1$, $B = 0.7$ and $0 < C \leq 0.1$ subject to the ABC flow (1.1) plus a small disturbance at order of magnitude 10^{-3} as the initial condition used when solving the NS and continuity equations (3.1) and (3.2), where T_{tran} denotes the time of transition occurrence.

as illustrated in figure 11, indicating that $T_{tran} \to +\infty$ as $C \to 0$. Hence, indeed the transition from laminar flow to turbulence should never occur when $C = 0$, which agrees with our numerical simulation in the case of $C = 0$ mentioned above. In all cases of $A = 1$, $B = 0.7$ and $0 < C \leq 0.43$ under consideration, it is found that all trajectories of the fluid particles starting from the randomly chosen 10 000 fluid particles are ultra-chaotic after the flow becomes fully turbulent. Besides, the smaller the number of ultra-chaotic particles at the beginning (corresponding to an unstable ABC flow with a smaller value of C), the longer the transition time of T_{tran}. In other words, more time is needed for all fluid particles to become ultra-chaotic at $t = T_{tran}$. The foregoing again suggests that a necessary condition of the occurrence of transition from laminar flow to turbulence is that nearly all fluid particles should move along ultra-chaotic trajectories.

Here, regarding the ultra-chaotic motion as a new property of fluid particle, we simply report some results of numerical experiments governed by (3.1) and (3.2) subject to periodic boundary conditions. Frankly speaking, it is not yet understood why almost all fluid particles should move along ultra-chaotic trajectories when the flow becomes fully turbulent: What happens to the trajectory property of fluid particles when the transition

from laminar flow to turbulence occurs, and so on? We firmly believe that the concept of ultra-chaos could enable us to gain new insight into viscous flows. We intend to pursue this in future work.

It should be emphasized that the transition from laminar flow to turbulence is a key problem in fluid mechanics. Hopefully, ultra-chaos as a new concept could provide us a completely new viewpoint to investigate and understand the mechanism of the transition to turbulence.

4. Concluding remarks and discussions

Due to the butterfly effect (Lorenz 1963), numerical noise (due to truncation error and round-off error) enlarges exponentially so that a computer-generated simulation of chaotic systems quickly becomes a mixture of a 'true' physical solution s and a 'false' numerical noise ε, which are mostly at the same order of magnitude. In practice, statistics of chaotic systems are usually calculated using such a mixture, i.e. $s + \varepsilon$, because there is no way to separate out the 'true' physical solution s. In fact, the statistics is based on the hypothesis

$$\langle s + \varepsilon \rangle = \langle s \rangle, \tag{4.1}$$

where $\langle \rangle$ is a statistical operator. Here, the numerical noise ε is in fact equivalent to a kind of small disturbances. Unfortunately, there exists no theoretical proof that the above hypothesis is always true in general.

By means of CNS (Liao 2009, 2013, 2014, 2017), one can gain reliable/convergent numerical simulations of chaotic systems over a long enough interval of time (Liao & Wang 2014; Li & Liao 2017; Lin *et al.* 2017; Hu & Liao 2020; Qin & Liao 2020; Liao & Qin 2022; Qin & Liao 2022; Yang *et al.* 2023), during which the 'false' numerical noise ε is much smaller than the 'true' physical solution s, say, $|\varepsilon| \ll |s|$, thus the influence of the numerical noise ε is negligible compared with the 'true' physical solution s. Hence, CNS can provide us, for the first time, with a nearly 'clean' computer-generated simulation of chaos in an interval of time long enough for statistics, which can be used as a benchmark solution since it is very close to the 'true' physical solution s. Therefore, CNS provides us with a useful tool by which to study accurately the influence of numerical noise on statistics of different types of chaotic systems (Hu & Liao 2020; Qin & Liao 2020; Liao & Qin 2022; Qin & Liao 2022; Yang *et al.* 2023).

Using CNS, it has been observed that the hypothesis $\langle s + \varepsilon \rangle = \langle s \rangle$ holds for many chaotic systems, whose statistics are stable to small disturbances. However, it has been found that statistics of some chaotic systems are indeed rather sensitive to small disturbances including artificial numerical noise (Hu & Liao 2020; Qin & Liao 2020, 2022; Yang *et al.* 2023), say, $\langle s + \varepsilon \rangle \neq \langle s \rangle$. Liao & Qin (2022) termed the former 'normal-chaos' and the latter 'ultra-chaos', respectively. The stability of trajectory and statistics of different types of dynamic systems is listed in table 1, which clearly indicates that an ultra-chaos is a higher disorder than a normal-chaos.

It is well known that the steady-state ABC flow, which satisfies the steady NS equations with a proper external force, has chaotic properties from a Lagrangian viewpoint. Naturally, it is worth investigating whether ultra-chaos exists in ABC flow, whether relationships hold between ultra-chaos and turbulence, and so on. In this paper, we illustrate that trajectories of many fluid particles in the steady-state ABC flow (1.1) are ultra-chaotic, in that their statistical properties are rather sensitive to tiny disturbances. Obviously, this kind of ultra-chaotic motion of fluid particles represents a higher disorder than normal-chaotic ones. We found that these two kinds of totally different chaos coexist widely and simultaneously in the steady-state ABC flow.

Besides, we discuss the difference between ultra-chaos and the high sensitivity of statistics to parameters, and also the relationships between ultra-chaos and Poincaré section, ultra-chaos and ergodicity, and so on. Unlike the high sensitivity of statistics to parameters, ultra-chaos focuses on the stability of statistics to very small disturbances. We have illustrated that certain model equations (such as the Lorenz-84 climate model with seasonal forcing) exhibit high sensitivity of statistics to parameters, even though all the statistics remain stable so that all the simulations involve either non-chaos or normal-chaos.

Furthermore, we discuss the possible relationship between the Poincaré section and normal/ultra-chaos. It is found that the normal-chaotic (starting) points (at $z = 0$) of the ABC flow correspond to elliptic islands (or KAM tori), but the ultra-chaotic ones correspond to the chaotic sea of the Poincaré section. It should be emphasized that, considering the fact that the Poincaré section has a close relationship with the KAM theory that is usually suitable for an integrable Hamiltonian system only, the new classification of chaos into ultra-chaos and normal-chaos is more general because of its validity for all dynamic systems, even if they are not Hamiltonian, and/or not integrable. Therefore, this new classification should have more general meaning.

In addition, we discuss possible relationships between ultra-chaos and non-ergodicity. According to Birkhoff (1931) and von Neumann (1932), time averages can be set equal to phase averages, provided the system is ergodic (i.e. metrically transitive) (Moore 2015). However, it is very difficult to seriously prove that a system is metrically transitive. It is an open question whether or not a normal-chaos corresponds to ergodicity and an ultra-chaos corresponds to non-ergodicity, respectively. Hopefully the classification of chaos into normal-chaos and ultra-chaos could provide us a simple and practical way to investigate ergodic property of various types of dynamic systems.

In order to study the possible relationships between ultra-chaos and turbulence, we numerically solve the NS and continuity equations (3.1) and (3.2) when $Re = 50$ using the ABC flow (for $A = 1$, $B = 0.7$ and various values of C) plus a small disturbance as the initial condition. It is found that the trajectories of nearly all fluid particles become ultra-chaotic after the transition from laminar to turbulent flow occurs. Our numerical facts strongly suggest that turbulence is likely to be related to ultra-chaotic trajectories of fluid particles, although the detailed mechanisms are presently unknown. Considering that the chaotic property of the ABC flow is essential for the development of turbulence (Dombre *et al.* 1986; Galloway & Frisch 1987; Podvigina & Pouquet 1994), we anticipate that the concept of ultra-chaos (Liao & Qin 2022) could lead to a better understanding of fluid chaos, Poincaré section, ergodicity/non-ergodicity, turbulence and their inter-relationships.

Author ORCIDs.
 Shijie Qin https://orcid.org/0000-0002-0809-1766;
 Shijun Liao https://orcid.org/0000-0002-2372-9502.

Author contributions. Liao conceived and designed the analysis and related concepts. Qin performed the computations. Both wrote the manuscript.

REFERENCES

ARNOLD, V.I. 1965 Sur la topologie des écoulements stationnaires des fluides parfaits. *C. R. Acad. Sci. Paris* **261**, 17–20.

ASHWIN, P., WIECZOREK, S., VITOLO, R. & COX, P. 2012 Tipping points in open systems: bifurcation, noise-induced and rate-dependent examples in the climate system. *Phil. Trans. R. Soc. Lond.* A **370** (1962), 1166–1184.

BIRKHOFF, G.D. 1931 Proof of the ergodic theorem. *Proc. Natl Acad. Sci. USA* **17** (12), 656–660.

BLAZEVSKI, D. & HALLER, G. 2014 Hyperbolic and elliptic transport barriers in three-dimensional unsteady flows. *Physica* D **273**, 46–62.

BROER, H., SIMÓ, C. & VITOLO, R. 2002 Bifurcations and strange attractors in the Lorenz-84 climate model with seasonal forcing. *Nonlinearity* **15** (4), 1205.

CHILDRESS, S. 1970 New solutions of the kinematic dynamo problem. *J. Maths Phys.* **11** (10), 3063–3076.

CRANE, L. 2017 Infamous three-body problem has over a thousand new solutions. *New Sci.* Available at: https://www.newscientist.com/article/2148074-infamous-three-body-problem-has-over-a-thousand-new-solutions/.

DIDOV, A.A. & ULEYSKY, M.YU. 2018a Analysis of stationary points and their bifurcations in the ABC-flow. *Appl. Maths Comput.* **330**, 56–64.

DIDOV, A.A. & ULEYSKY, M.YU. 2018b Nonlinear resonances in the ABC-flow. *Chaos* **28** (1), 013123.

DOMBRE, T., FRISCH, U., GREENE, J.M., HÉNON, M., MEHR, A. & SOWARD, A.M. 1986 Chaotic streamlines in the ABC flows. *J. Fluid Mech.* **167**, 353–391.

FINN, J.M. & OTT, E. 1988 Chaotic flows and fast magnetic dynamos. *Phys. Fluids* **31** (10), 2992–3011.

GALLOWAY, D. & FRISCH, U. 1986 Dynamo action in a family of flows with chaotic streamlines. *Geophys. Astrophys. Fluid Dyn.* **36** (1), 53–83.

GALLOWAY, D. & FRISCH, U. 1987 A note on the stability of a family of space-periodic Beltrami flows. *J. Fluid Mech.* **180**, 557–564.

GAO, S., TAO, L., TIAN, X. & YANG, J. 2018 Flow around an inclined circular disk. *J. Fluid Mech.* **851**, 687–714.

HU, T. & LIAO, S. 2020 On the risks of using double precision in numerical simulations of spatio-temporal chaos. *J. Comput. Phys.* **418**, 109629.

KUZNETSOV, L. & ZASLAVSKY, G.M. 2000 Passive particle transport in three-vortex flow. *Phys. Rev.* E **61** (4), 3777–3792.

LEE, W.-K., BORTHWICK, A.G.L. & TAYLOR, P.H. 2014 Wind-induced chaotic mixing in a two-layer density-stratified shallow flow. *J. Hydraul. Res.* **52** (2), 219–227.

LI, T.Y. & YORKE, J.A. 1975 Period three implies chaos. *Am. Math. Mon.* **82** (10), 985–992.

LI, X., JING, Y. & LIAO, S. 2018 Over a thousand new periodic orbits of a planar three-body system with unequal masses. *Publ. Astron. Soc. Japan* **70** (4), 64.

LI, X. & LIAO, S. 2017 More than six hundred new families of Newtonian periodic planar collisionless three-body orbits. *Sci. China Phys. Mech.* **60** (12), 129511.

LI, X. & LIAO, S. 2019 Collisionless periodic orbits in the free-fall three-body problem. *New Astron.* **70**, 22–26.

LI, Y.C., HO, R.D.J.G., BERERA, A. & FENG, Z.C. 2020 Superfast amplification and superfast nonlinear saturation of perturbations as a mechanism of turbulence. *J. Fluid Mech.* **904**, A27.

LIAO, S. 2009 On the reliability of computed chaotic solutions of non-linear differential equations. *Tellus* A **61** (4), 550–564.

LIAO, S. 2013 On the numerical simulation of propagation of micro-level inherent uncertainty for chaotic dynamic systems. *Chaos, Solitons Fractals* **47**, 1–12.

LIAO, S. 2014 Physical limit of prediction for chaotic motion of three-body problem. *Commun. Nonlinear Sci. Numer. Simul.* **19** (3), 601–616.

LIAO, S.J. 2017 On the clean numerical simulation (CNS) of chaotic dynamic systems. *J. Hydrodyn.* **29** (5), 729–747.

LIAO, S. & QIN, S. 2022 Ultra-chaos: an insurmountable objective obstacle of reproducibility and replication. *Adv. Appl. Maths Mech.* **14** (4), 799–815.

LIAO, S. & WANG, P. 2014 On the mathematically reliable long-term simulation of chaotic solutions of Lorenz equation in the interval [0, 10 000]. *Sci. China Phys. Mech.* **57** (2), 330–335.

LIN, Z., WANG, L. & LIAO, S. 2017 On the origin of intrinsic randomness of Rayleigh–Bénard turbulence. *Sci. China Phys. Mech.* **60** (1), 1–13.

LORENZ, E.N. 1963 Deterministic nonperiodic flow. *J. Atmos. Sci.* **20** (2), 130–141.

LORENZ, E.N. 1989 Computational chaos-a prelude to computational instability. *Physica* D **35** (3), 299–317.

LORENZ, E.N. 1993 *The Essence of Chaos*. University of Washington Press.

LORENZ, E.N. 2006 Computational periodicity as observed in a simple system. *Tellus* A **58** (5), 549–557.

LUCARINI, V. & BÓDAI, T. 2019 Transitions across melancholia states in a climate model: reconciling the deterministic and stochastic points of view. *Phys. Rev. Lett.* **122** (15), 158701.

LUKES-GERAKOPOULOS, G., VOGLIS, N. & EFTHYMIOPOULOS, C. 2008 The production of Tsallis entropy in the limit of weak chaos and a new indicator of chaoticity. *Physica* A **387** (8), 1907–1925.

MEZIĆ, I. 2002 An extension of Prandtl–Batchelor theory and consequences for chaotic advection. *Phys. Fluids* **14** (9), L61–L64.

MOFFATT, H.K. & PROCTOR, M.R.E. 1985 Topological constraints associated with fast dynamo action. *J. Fluid Mech.* **154**, 493–507.

MOORE, C.C. 2015 Ergodic theorem, ergodic theory, and statistical mechanics. *Proc. Natl Acad. Sci. USA* **112** (7), 1907–1911.

VON NEUMANN, J.V. 1932 Proof of the quasi-ergodic hypothesis. *Proc. Natl Acad. Sci. USA* **18** (1), 70–82.

NEWTON, I. 1687 *Philosophiae Naturalis Principia Mathematica*. Royal Society.

OYANARTE, P. 1990 MP – a multiple precision package. *Comput. Phys. Commun.* **59** (2), 345–358.

PARKER, T.S. & CHUA, L.O. 1989 Practical numerical algorithms for chaotic systems. *Maths Comput.* **66** (1), 125–128.

PETER, S. 1998 *Explaining Chaos*. Cambridge University Press.

PODVIGINA, O., ASHWIN, P. & HAWKER, D. 2006 Modelling instability of ABC flow using a mode interaction between steady and Hopf bifurcations with rotational symmetries of the cube. *Physica* D **215** (1), 62–79.

PODVIGINA, O. & POUQUET, A. 1994 On the non-linear stability of the 1 : 1 : 1 ABC flow. *Physica* D **75** (4), 471–508.

POINCARÉ, H. 1890 Sur le problème des trois corps et les équations de la dynamique. *Acta Mathematica* **13** (1), A3–A270.

POPE, S.B. 2001 *Turbulent Flows*. IOP.

QIN, S. & LIAO, S. 2020 Influence of numerical noises on computer-generated simulation of spatio-temporal chaos. *Chaos, Solitons Fractals* **136**, 109790.

QIN, S. & LIAO, S. 2022 Large-scale influence of numerical noises as artificial stochastic disturbances on a sustained turbulence. *J. Fluid Mech.* **948**, A7.

RUELLE, D. & TAKENS, F. 1971 On the nature of turbulence. *Commun. Math. Phys.* **20** (3), 167–192.

SKOKOS, CH. 2001 Alignment indices: a new, simple method for determining the ordered or chaotic nature of orbits. *J. Phys.* A*: Math. Gen.* **34** (47), 10029–10043.

ŚLIWIAK, A.A., CHANDRAMOORTHY, N. & WANG, Q. 2021 Computational assessment of smooth and rough parameter dependence of statistics in chaotic dynamical systems. *Commun. Nonlinear Sci. Numer. Simul.* **101**, 105906.

SPROTT, J.C. 2010 *Elegant Chaos: Algebraically Simple Chaotic Flows*. World Scientific.

STANKEVICH, N., KAZAKOV, A. & GONCHENKO, S. 2020 Scenarios of hyperchaos occurrence in 4D Rössler system. *Chaos* **30**, 123129.

TEIXEIRA, J., REYNOLDS, C.A. & JUDD, K. 2007 Time step sensitivity of nonlinear atmospheric models: numerical convergence, truncation error growth, and ensemble design. *J. Atmos. Sci.* **64** (1), 175–189.

VAN GORDER, R.A. 2013 Shilnikov chaos in the 4D Lorenz–Stenflo system modeling the time evolution of nonlinear acoustic-gravity waves in a rotating atmosphere. *Nonlinear Dyn.* **72** (4), 837–851.

WHYTE, C. 2018 Watch the weird new solutions to the baffling three-body problem. *New Sci.* Available at: https://www.newscientist.com/article/2170161-watch-the-weird-new-solutions-to-the-baffling-three-body-problem/.

XU, T., LI, J., LI, Z. & LIAO, S. 2021 Accurate predictions of chaotic motion of a free fall disk. *Phys. Fluids* **33** (3), 037111.

YANG, Y., QIN, S. & LIAO, S. 2023 Ultra-chaos of a mobile robot: a higher disorder than normal-chaos. *Chaos, Solitons Fractals* **167**, 113037.